Investigation of Local Hemodynamics Effect in Disturbed Flow Interactions

Abdullah Alshorman [*]

Al-Balqa` Applied University – Al-Huson University College - Mechanical Engineering Department, P.O.Box 50, Al-Huson 21510 – Irbid - Jordan

Abstract

Physiologically, blood flow path has different patterns of geometry, shapes, size and structure within the cardiovascular system. This includes branching, bifurcation and curvature of blood vessels and other cardiovascular components.

Accordingly, the blood micro interactions with the lining layer (Endothelium Layer) of blood vessels and surrounding surfaces are strongly depend on blood constitutions, mechanical properties of endothelial layer and the geometry of blood pathways. This demonstrating the importance of local hemodynamics in controlling disturbed flow interactions, which include leukocytes aggregation and platelets adhesion.

In the present study, a numerical simulation of blood-surface interactions are performed to investigate the complicated behavior of blood flow and how the local hemodynamics control the adhesion and rolling processes around a stagnation point at branching and curvature locations within cardiovascular system. These investigations are carried out under effect of variable shear stress, and different timing of secondary adhesion technique.

The results showed that the discontinuity in the hemodynamic flow enhances cell adhesion under low shear rate at and downstream the disturbed portion in the flow (i.e., stenosis flow). Also, cell prefers to adhere to the surface between the discontinuity and little bit further the stagnation point, but the maximum tendency for adhesion is before the stagnation point, which synchronized with the lowest value of shear rate. However, at higher shear rate (i.e., 19.66 s-1) the cell will roll slowly for short time before its rolling velocity gradually increases to reach a maximum value when the shear rate gets higher.

Keywords: *Disturbed blood flow, stagnation point, shear stress, hemodynamics.*

Nomenclatures

a_c	Cell radius
a_{co}	Characteristics cell radius (Reference value)
$A(\theta,\phi)$	Individual grid area of the receptors over the cell surface
C_x	Distance from the step
C_y	Distance between the cell center and the vessel surface
F_b	The bonding force
F_{bi}	The bonding force in Cartesian Coordinate (i=x,y and z)
F_{flx}	Hemodynamic force x-direction (Fluid force)
F_{fly}	Hemodynamic force y-direction (Fluid force)
f_k	Fraction of bond strain that is dedicated to bond dissociation, (fractional spring slippage)
F_s	Function of $(a_c + h)/a_c$
G	Shear rate
G_o	Characteristic shear rate (Reference value)
h	The minimum distance between the cell and the surface
I	Mass moment of inertia of the cell
K_B	Boltzmann constant
K_b	Bond breakage constant
K_f	The intrinsic bond formation rate constant
K_{ro}	The intrinsic bond breakage rate constant
L_b	bond length
m	mass of the cell
M_{bz}	Moment of the bond force in z-direction
n_{Ro}	Receptors of density while the
n_{Lo}	Ligands of density
n_B	Bonds of density
S	Stiffness constant
S_{ts}	Transition state spring constant,
T	The temperature
T_{max}	Overall time of simulation
V_{cell}	Cell velocity
V_f	Velocity of the fluid with respect to the cell velocity V_{cell}
δt	Time step
δc_i	Indices of the cell center in Cartesian Coordinate (i=x,y and z)
λ	Stressed bond length
λ_o	Equilibrium (unstressed) bond length
μ	The fluid dynamic viscosity
Ω_i	The three components of rotational velocity in Cartesian Coordinate (i=x,y and z)
ρ	Fluid density
τ	Dimensionless time

* Corresponding author e-mail: alshormana@asme.org.

Anchoring of blood cells to the surface of the blood vessel starts by the migration of cell from the blood stream toward the vessel surface; this may be followed by primary adhesion, rolling or permanent adhesion. These processes are essential events in physiological adhesion for instance Leukocyte accumulation during inflammation, tumor cell metastasis and thrombus formation [1]. However, adhesion and aggregation of platelets and neutrophils to each other and to blood vessel wall are critical events in inflammation and thrombosis, and are relevant to patients with stroke, acute myocardial infarction and coronary angioplasty [2, 3].

Under flow conditions, cell adhesion initiates by cell departure from the main bloodstream toward the vessel wall (cell capture), and then the cell slow rolling takes place (adhesive rolling) before the permanent adhesion happens (secondary adhesion). The driving force for rolling is the hydrodynamic force of the blood stream (hemodynamic force) acting on the adherent cell; rapid formation and breakage of adhesive bonds are required for the adhesive contact between the blood cell and the vessel wall to be maintained and to be translated along the wall during rolling [4,5]. On the way to inflammatory sites, neutrophils attach to and roll on endothelium before their firm arrest and diapendesis. The attachment and rolling of neutrophils are mediated by selectins (L-selectin on neutrophils; P-selectin and E-selectin on endothelium) and their carbohydrate ligands [6].

Fundamentally, cell adhesion/rolling depend on many parameters that are related to the flow conditions, cellular properties, bond characteristics, and interactions activity of the lining layer of the blood vessel (i.e., endothelium layer). Mainly, flow parameters include the flowing path, properties of the working fluid (i.e., blood or plasma), type of flow (laminar and turbulence levels and vessel size and shape), and local hemodynamics. The vascular endothelium cell is subjected at all time to shear forces that act on its surface and has an important role in regulating cell structure in endothelium and cardiac myocytes as a result of flow of viscous blood [7]. However, the viscous effect of blood has an important role in hemodynamics of blood stream, especially at stagnation points (zero velocity point) through the blood flow and at the disturbed portion (the discontinuity in the flow) [8].

The hemodynamic force depends mainly on the rate of shear and on the blood rheology. In addition to hemodynamic force, cell receptors and surface legends densities (site densities) have a crucial role in cell adhesion and rolling. However, the adhesion of cells to surfaces under conditions of flow represents a balance between physical and chemical forces. The chemical bonding force delivered by the receptor-ligand pair balances the hydrodynamic forces on the cell. This chemical bonding force is derived from the numbers and strength of adhesive linkages between cell and surface, which results from the properties of adhesion molecules [9, 10].

In the light of the above, it is important, therefore, to fully understand the mechanisms of fluid cell, capture, rolling and permanent adhesion under flow conditions. Of particular relevance is the role of local hemodynamics of blood flow in the cell-surface interactions. However, a fundamental quantitative understanding of cellular behavior can lead to better understanding of in vivo phenomena.

Accordingly, this study makes steps towards elucidation of the cell-surface interactions under flow conditions, such that a three-dimensional (3D) computational model was developed to simulate and investigate the effect of local blood hemodynamics in the cell adhesion and motion over the endothelium layer at the bifurcation sites of the cardiovascular system.

2. Methods and Model Development

The details of the biodynamical model and the coordinate axes appear through Figures 1-3. In this model, the blood cell (i.e., Leukocytes or neutrophils) is modeled to be an inflexible sphere of radius a_c covered by uniformly distributed receptors of density $[n_{Ro}]$ while the substrate (i.e., Endothelium layer) has ligands of density $[n_{Lo}]$. The resulting receptors-ligands combination (bonds)- within the contact zone- are modeled as Hookean springs with stiffness constant of S and equilibrium (unstressed) bond length of λ_o, while the stressed bond length is represented as λ.

Within the contact zone, the rate of bond formation constant (K_f) and breakage constant (K_b) are determined using the expressions suggested by Bell model [11] which is modified by Dembo *et al.*, 1988 [12]:

$$K_f = K_{fo} \exp(-S_{ts}(\lambda - \lambda_o)^2 / 2 K_BT) \qquad (1)$$

$$K_r = K_{bo} \exp(f_k S (\lambda - \lambda_o)^2 / 2K_BT) \qquad (2)$$

Here λ is the bond length (the magnitude of the vector of Eqn.1), f_k is the fraction of bond strain that is dedicated to bond dissociation, and is also known as the fractional spring slippage, and is given by $f_k = [(S - S_{ts}) / S]$. The term (K_B T) is product of the Boltzmann constant and temperature, S is the spring constant, S_{ts} is the transition state spring constant, K_{fo} and K_{ro} are the intrinsic bond formation and breakage rate constants [1,13,14].

The bonding force F_b will depend on the deflection of the bond length *($\lambda - \lambda_o$)*, which is related to the (x,y,z) coordinates of the tether on both the cell $L_1(x_1,y_1,z_1)$ and that on the substrate $L_2(x_2,y_2,z_2)$, such that F_b, L_1 and L_2 are vector quantities. The vectors L_1 and L_2 change with time as a result of cell rotation and translation, so the bond length at each location can be described by a time varying vector:

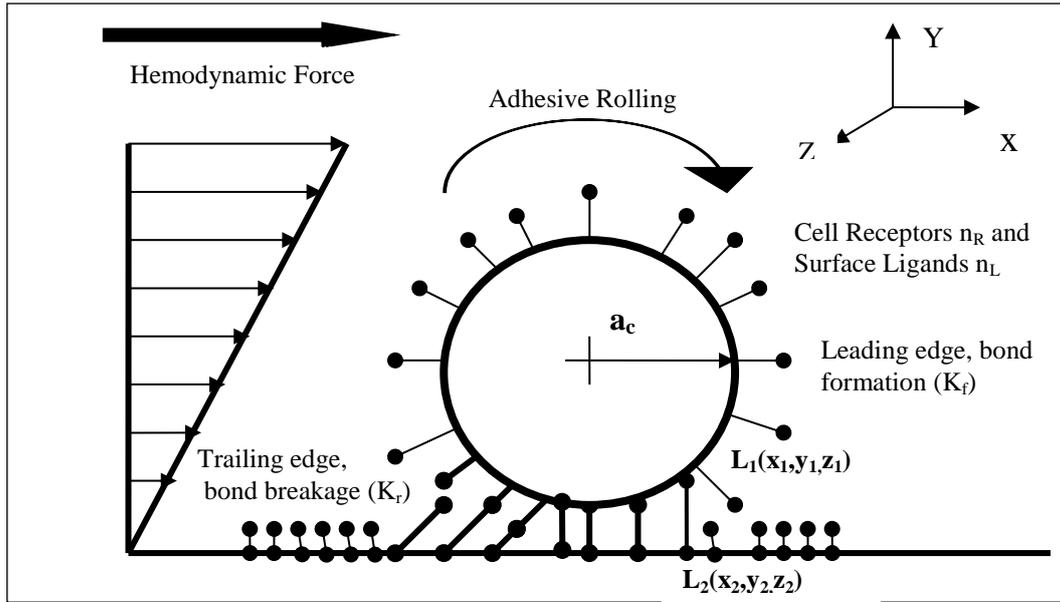$$L_b = L_2 - \mathbf{L_1} \qquad (3)$$

Figure 1. The cell is modelled as a sphere of radius a_c, covered with the receptors with a density of $[n_R]$, while the ligands covered the substrate at a density of $[n_L]$. Rolling occurs when the bonds at the trailing edge of the cell start to break
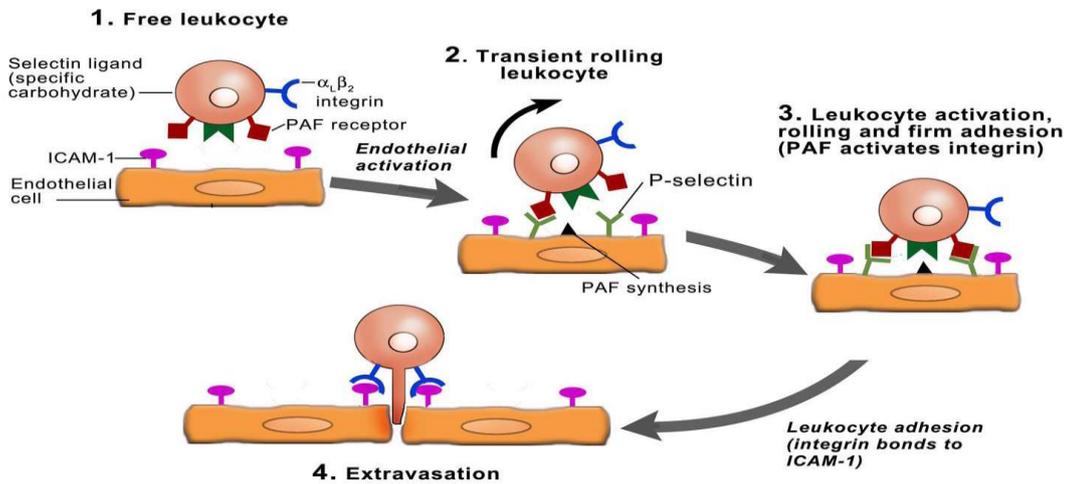

Figure 2. The four steps of cell adhesion under effects of shear effects [15]

In the contact region, ligands react with receptors at rate of bond formation (K_f) to form bonds of density n_B, so the rate of bond formation $\dfrac{dn_B}{dt}$ is given by:

$$\frac{dn_B}{dt} = K_f\, n_R\, n_L\; -\; K_b\, n_B \qquad (4)$$

Where n_B, n_L and n_R are the density in [number of sites/μm^2] of the bond, ligand and receptor, respectively.

Accordingly, the bond force can be resolved in each direction F_{bx}, F_{by} and F_{bz}, and the associated torques can also be calculated using the above appropriate parameters; subsequently, the single bond force in each Cartesian direction can be expressed as:

$$F_{bx} = S\, L_{bx} \left(1 - \frac{L_{bo}}{L_b} \right) \qquad (5)$$

$$F_{by} = S\, L_{by} \left(1 - \frac{L_{bo}}{L_b} \right) \qquad (6)$$

$$F_{bz} = 0.0 \qquad (7)$$

Here, F_{bz} equals zero since there is no cell motion in z-direction and λ_z doesn't change, while the total bond forces take the following forms:

$$\Sigma F_{bx} = S\; \lambda_x \left(1 - \frac{\lambda_o}{\lambda} \right) n_B\, A(\theta,\phi\ ) \qquad (8)$$

$$\Sigma F_{by} = S\; \lambda_y \left(1 - \frac{\lambda_o}{\lambda} \right) n_B\, A(\theta,\phi\ ) \qquad (9)$$

$$\Sigma M_{bz} = \lambda_x\;\; y_1\,(\theta,\phi\ ) \; + \; \lambda_y\;\; x_1\,(\theta,\phi\ ) \qquad (10)$$

Here, n_B is the bond density, and $A(\theta,\phi\ )$ is the individual grid area of the receptors over the cell surface (Fig. 3). Fig. 3 shows the resultant of the bonds in each grid of the cell surface, such that the resultant summation of the individual bonds is located at the center of the grid. Also, $x_1\,(\theta,\phi)$ and $y_1\,(\theta,\phi)$ are the location distance of the receptors on the cell surface in x and y directions.
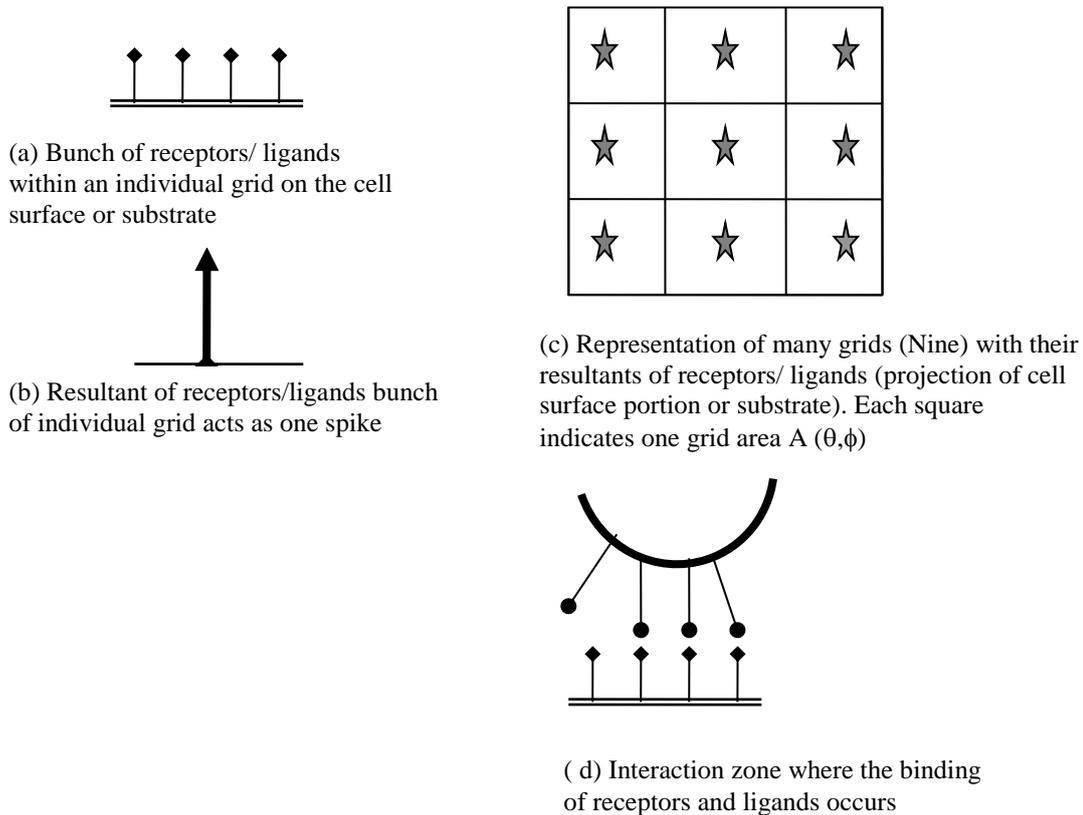
(a) Bunch of receptors/ ligands within an individual grid on the cell surface or substrate

(b) Resultant of receptors/ligands bunch of individual grid acts as one spike

(c) Representation of many grids (Nine) with their resultants of receptors/ ligands (projection of cell surface portion or substrate). Each square indicates one grid area A (θ,ϕ)

(d) Interaction zone where the binding of receptors and ligands occurs

Figure 3. Representation of the spherical grid over the cell surface / substrate surface, such that each small square indicates one individual grid area A(θ, ϕ) and the effect of receptors/ligands resultant acting at the centres of the small squares

The driving effect on the cell is the hydrodynamic (hemodynamic) force such that the effects of bond keep opposing the hemodynamic contribution to achieve the stability of adhesive rolling. However, rolling occurs as long as the hemodynamic force is greater than the integrated effect of bond forces, while permanent adhesion is associated with the dominant role of bond forces against the driving effect. Particularly, hemodynamic force can be derived to take the following form [1, 14, 16, 17, 18]:

$$F_{flx} = 6\,\pi\,\mu\,a_c^2\,(\,G - V_x\,/\,d_y\,)\,F_s \tag{11}$$

$$F_{fly} = -\,6\,\pi\,\mu\,a_c\,V_x\,F_s \tag{12}$$

where G is shear rate in x-direction, μ is the fluid dynamic viscosity, F_s is a function of $(a_c + h)/a_c$ such that h is the minimum distance between the cell and the surface, the value used for F_s is (1.7) (Goldman *et al*., 1967), V_x & V_y are the velocity of the cell in x and y direction, and C_y is the distance between the cell center and surface.

As a result of net effects of hemodynamic and bond forces the cell moves at rolling velocities V_x, V_y and V_ϕ under certain values of bond formation and dissociation rates constants (K_f and K_b). The motion of the cell was determined by solving Newton's law of motion, balancing fluid and bond forces with inertia, such that:

$$\Sigma Fx = \Sigma Fbx + Fflx \tag{13}$$

$$\Sigma F_y = \Sigma F_{by} + F_{fly} \tag{14}$$

Here ΣF_{bx} and ΣF_{by} are determined by Eqns. 8 & 9, while the fluid forces F_{fl} can be calculated using Eqns. 11

& 12 and the relative velocity of the fluid V_f with respect to the cell velocity V_{cell} (i.e., $V_f - V_{cell}$):

$$F_{fl} = 6\,\pi\,\mu\,a_c^2\,[V_f - V_{cell}]\,F_s \tag{15}$$

Fluid velocity V_f can be evaluated as a function of shear rate G and the distance between the cell center and the surface C_y, so:

$$V_f = G\,C_y \tag{16}$$

Then

$$V_f - V_{cell\_i} = G - \frac{V_{cell\_i}}{C_y}, \quad i = x,y,z \text{ or } \phi \tag{17}$$

The cell velocity components (V_x, V_y, V_ϕ) are expressed by Eqn. 24 below, while the fluid force components are:

$$F_{flx} = 6\,\pi\,\mu\,a_c^2\,\left[\,G - \left(\frac{\partial c_x}{\partial t C_y}\right)\right]\,F_s \tag{18}$$

$$F_{fly} = -\,6\,\pi\,\mu\,a_c^2\,\left(\frac{\partial c_y}{\partial t C_y}\right)\,F_s^{*} \tag{19}$$

Where μ is the dynamic viscosity of plasma, which is equal to 1-2 centi-poise (cp.) (i.e., $\mu = 1\times10^{-6}$ - 2×10^{-6} g/μm.s) [10,22,29,32,33], G is the shear rate, C_y is the total height of the cell center from the substrate such that $C_y = \Sigma\,\delta c_y$, and F^{*} is function of the ratio of distance between cell center and substrate h and cell radius a_c, ($F^{*} \sim 1+(9/16)(a_c/h)$ for small (h/a_c). Numerical values of h/a_c

and their associated values of F^* are introduced and tabulated by Goldman *et al.*, 1967, F^* ranges from 1.0 to 1.7005). The shear-induced force approach finite limits as the cell contacts the wall, thus $F^* = 1.7005$ for the limiting case $h/a_c = 1.0$, [16, 17, 23, 24, 25].

Consequently, the general form of equation of cell motion can be expressed in the following form (Eulerian approximation method):

$$\sum F = m \frac{\left(\partial c_{i+1} - \partial c_i \right)}{\partial t^2}, \; i = x,y,z \; or \; \phi \qquad (20)$$

Based on Eqn. 20, cell motion can be characterized by the indices of the cell center in each Cartesian co-ordinate δc_x, δc_y and δc_ϕ that are governed by Eqns.(21-23).

$$\delta c_{x+1} = \frac{(\partial t)^2}{m} \sum F_x + \delta c_x \qquad (21)$$

$$\delta c_{y+1} = \frac{(\partial t)^2}{m} \sum F_y + \delta c_y \qquad (22)$$

$$\delta c_{\phi+1} = \frac{(\partial t)^2}{I} \sum M_z + \delta c_\phi \qquad (23)$$

Where δc_i is the infinitesimal change in cell center position in i-direction (i = x,y & z or ϕ) at time t, while δc_{i+1} is that at time $t + \delta t$ and I is the mass moment of inertia of the cell as it is modeled as sphere.

The cell moves in both translation and rotation modes with three different components of translation velocity in each Cartesian co-ordinate V_x, V_y and V_z, while Ω_x, Ω_y and Ω_z are the three components of rotational velocity. According to the model, V_z, Ω_x and Ω_y are equal zero since there is no translation in z-direction and no rotation about x and y axis. Obviously, the cell translates in the x and y directions at V_x and V_y and rolls at Ω_z or V_ϕ about z-direction (V_ϕ is considered instead of Ω_z for notation consistency). These instantaneous velocity components are modeled to be in the following form:

$$V_i = \frac{\partial c_i}{\partial t}, \; i=x,y,\phi \qquad (24)$$

The cell rolling velocity is evaluated at each time step δt for the whole different stages of adhesion and rolling processes within the time of simulation T_{max}.

3. The Main Features of Flow at Localized Zones under Variable Shear Rate

To highlight the characteristics of the local hemodynamics of blood flow at localized sites (i.e., branching, contraction expansion, tapering), the path flow over the step is investigated since it could be considered as an interpretation for these restricted locations.

The flow over the step has a complicated nature due to discontinuity in the path of flow, circulation and back flow downstream the step, also this type of flow can be considered as primary related to stenosis flow and flow through branching vessels, such as the blood flow over cell adherent accumulation (plaque), or disturbed vessel flow respectively.

The schematic diagram and stream lines of step flow are shown in Figs. 4 and 5, where cell adhesion occurs around the stagnation point and back flow in the circulation zone. While the non-dimensional and the dimensional shear rate distribution over the distance from the step are illustrated in Figs. 6 and 7, respectively. This distribution is for Reynolds number (Re) of 28.5, dynamic viscosity of 7×10^{-7} g/μm-s and 300 μm for the step height.

According to Fig. 6, the shear rate starts from zero at the beginning of the step then decreases in negative to reach its peak negative value after which it increases to come back to zero value at the stagnation point at the non-dimensional distance (C_x / a_c) of 162. Here, C_x is the position distances of the cell along x axis, while a_c is the characteristics cell radius. Just slightly next the stagnation point, the shear rate changes sharply from zero up to its maximum value before it takes its constant value ($G/G_o = 1.0$) which is the used characteristics value (G_o) for the non-dimensionalizing process.
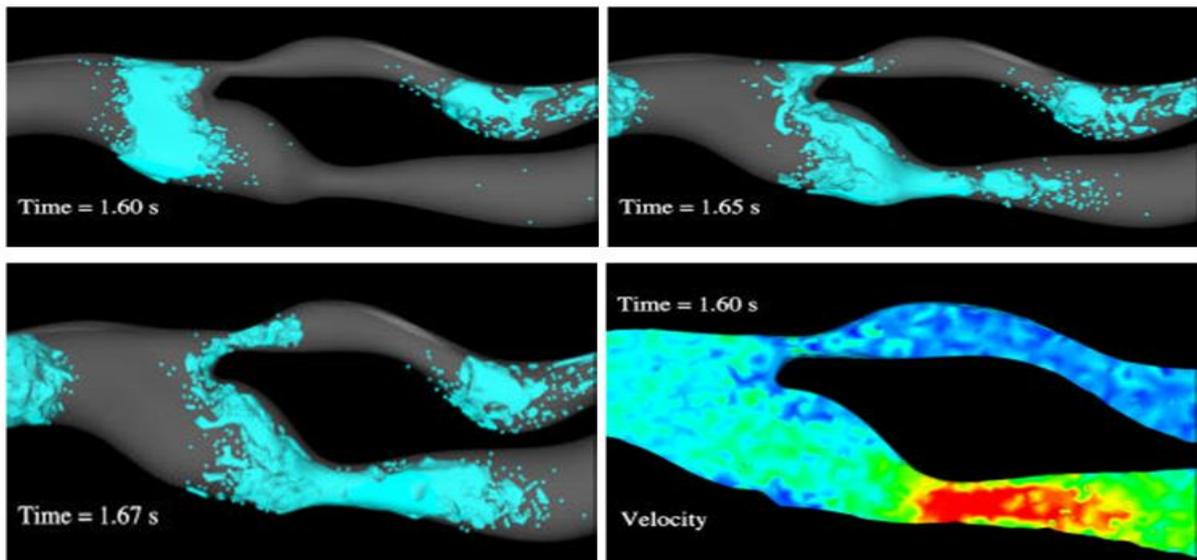

Figure 4-a. CFD of bifurcation flow at different times indicating stagnation points and adhesion regions [26].
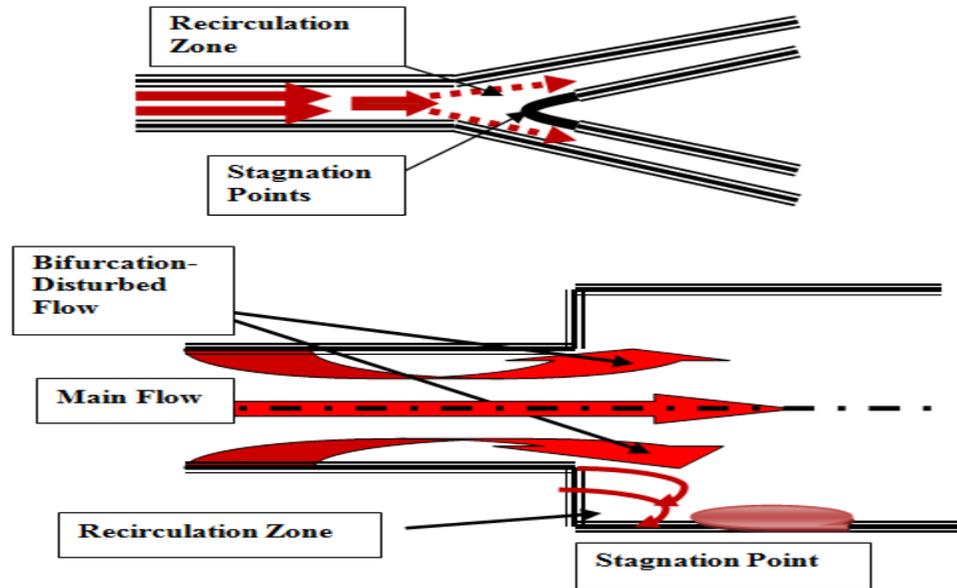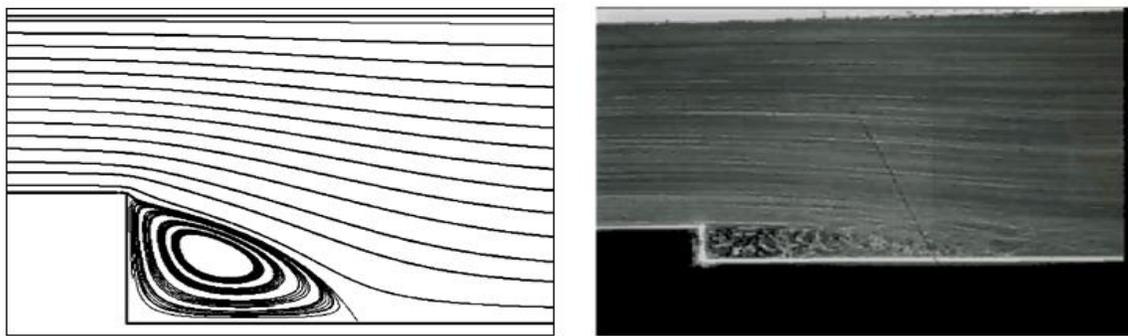
Figure 4-b. Disturbed flow representation: Arteries bifurcation, step flow, recirculation zone and stagnation point

a. **CFD visualization**

b. **Flow visualization [27]**

Figure 5. Disturbed step flow field: Circulation zone with back flow, stagnation point and recirculation
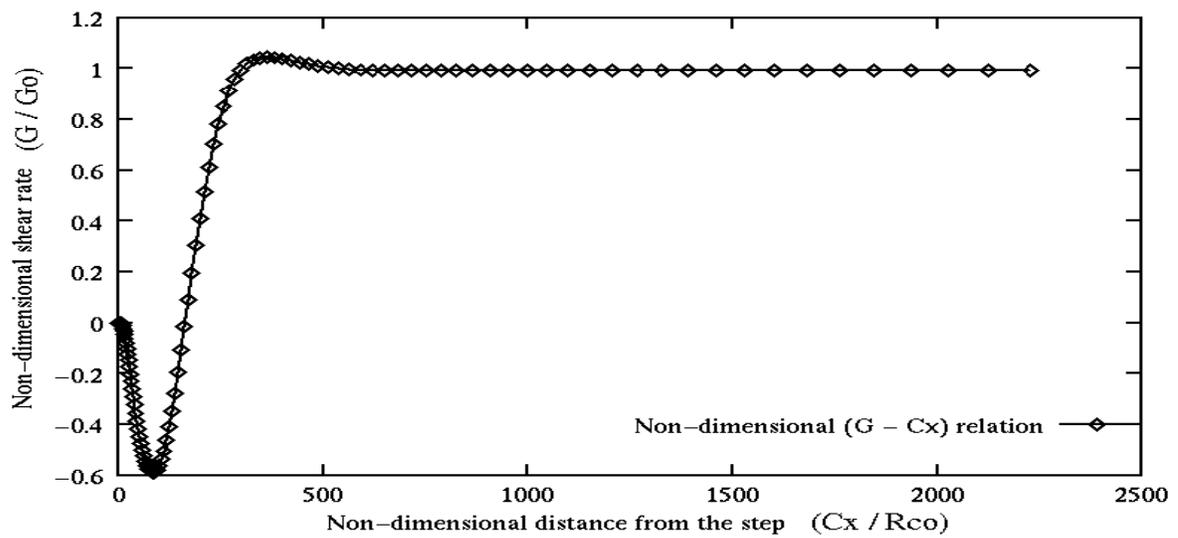

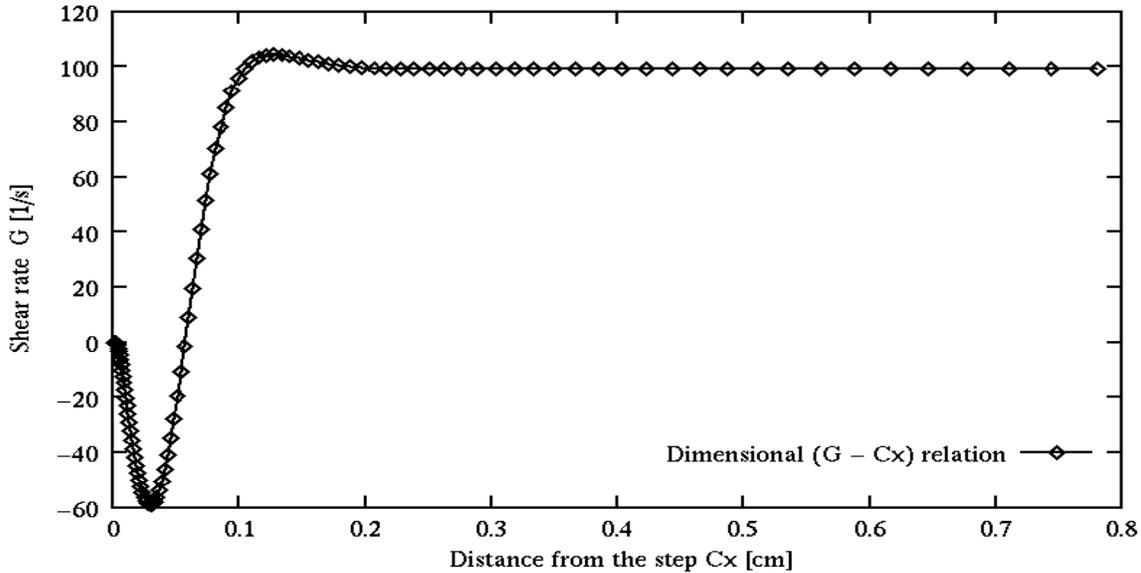**Figure 6.** Non-dimensional shear rate distributions over the non-dimensional distance from the step

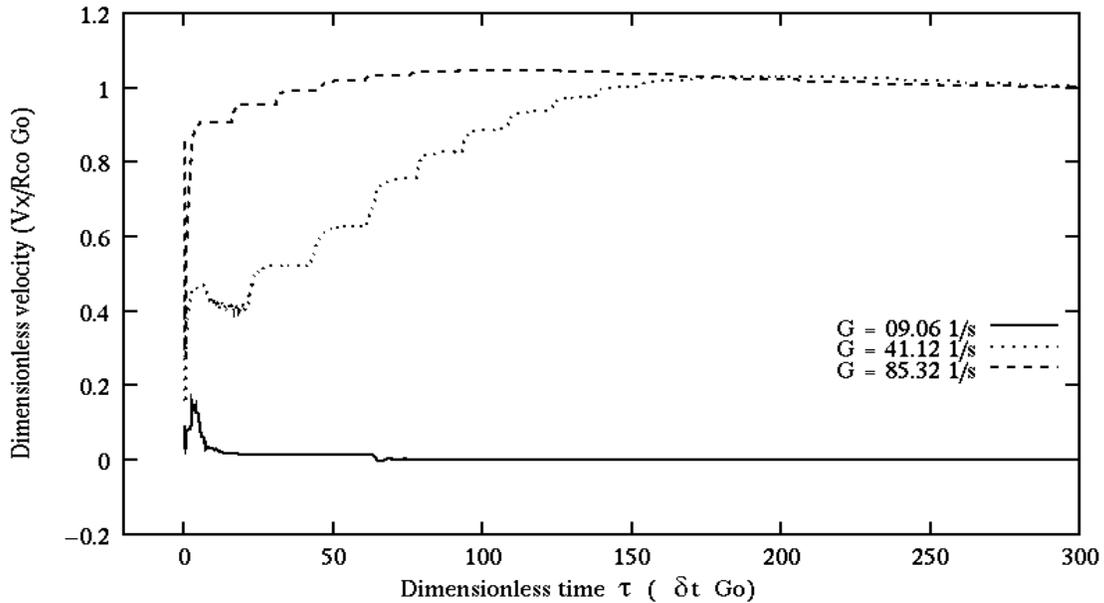**Figure 7.** Shear rate distributions over the distance from the step (dimensional values)

Figure 8. Cell capture, rolling and secondary adhesion under range of positive variable shear rate (after the stagnation point location)

4. Results and Discussion

In the present study, an instantaneous-continuous reading of shear rate is performed at each cell position in each simulation run for the entire data of Fig. 6. Set of simulations were executed to analyze the features of cell capture, rolling and adhesion under the conditions of disturbed flow. The setting of input parameters of simulation are listed in Table 1 and the results are presented through Figs. 8 –10 and 12-13.

The results demonstrate the type of cell behavior within the effective range of shear rate (capture, rolling or adhesion) and show the direction of cell motion under the conditions of the current flow.

Figure 8 shows the cell capture rolling and secondary adhesion at different starting position with positive initial shear rates of 9.06, 41.12 and 85.32 s[1].

It can be noted that the cell has the three stages of cell adhesion (capture, rolling and secondary adhesion) when it starts at G = 9.06 (position of C_x/a_c of 169.7). But at higher shear rate (i.e., 41.12 and 85.32 s^{-1}) the cell will roll slowly for short time before its rolling velocity gradually increases to reach a maximum value

as the shear rate gets higher (no adhesion and continuous rolling).

On the other hand, under most of negative shear rates (upstream of the stagnation point), the captured cell tends to adhere and stop rolling after certain period of time as demonstrated in Fig. 9. This indicates that cells within the effect of these shear rates ranges prefer adhesion after short slow rolling. As expected the cell in this area of flow, follows in the direction of shear rate, so its short rolling was toward the step to the left of the stagnation point, where the adhesion takes place under the negative shear rates.

In their experimental study, Skilbeck et al. [28] reported that within the circulation zone, wall shear stress was never so high as to disallow adhesion. This was not the case downstream the reattachment point in a high shear channel. Adhesion quickly dropped off beyond this point as wall shear stress increased. It was difficult to ascertain how many of cells that adhered beyond the reattachment point had been released from the vortex and how many had followed the streamlines that ran close to the wall upstream of the step and stayed downstream. Both types of attachment could be observed to occur occasionally.

To explore the cellular behavior downstream the step, more simulations were executed for different starting locations with dissimilar shear rates using the listed data of Table 1. The results of this simulation analysis are presented in Fig. 10.

By looking at Fig.10, it can be noted that cell adhesion is dominant within the distance between the step and the stagnation point (i.e., $C_x/a_c \leq 162$), the cells in this range roll shortly in the direction of shear rate (to the left) then adhere to the surface to form the whole/main part of the adhesion length. The cell keeps on zero rolling velocity at the stagnation point ($C_x/a_c = 162$), where no any previous rolling takes place, however as the starting location become far from the stagnation point under negative shear rate, the cell had short rolling before its permanent adhesion. Nevertheless, at the edge of the step the situation is considerably similar to that at the stagnation point.

On the other hand, under higher shear rate (to the right of stagnation point) the chance for adhesion decreases as the driving force (hemodynamic force) enlarges to enhance rolling. But at the closer locations ($C_x/a_c = 178.28$), to the right of the stagnation point, cells tend to adhere for certain time before the drag force promote them for fast rolling (other end of the adhesion length).

Three conclusions can be assigned based on these findings: First, the discontinuity in the hemodynamic flow enhances cell adhesion under low shear rate at and downstream the disturbed portion in the flow (i.e., stenosis flow). Second, cell prefers to adhere to the surface between the discontinuity and little bit further the stagnation point, but the maximum tendency for adhesion is before the stagnation point, which synchronized with the lowest value of shear rate. This adhesion vanishes just further to the stagnation point where cell starts rolling at different velocities, as the shear rate gets higher. Third, after certain limit of shear rate the cell starts to roll with its maximum rolling velocity when shear is not constant; it increases with location to reach the maximum limit, where the maximum stream velocity takes place.

Based on the above situation, it is possible to determine the adhesion length around the stagnation point and the shear rate limit that allow for adhesion as explained in the next sections.

Table 1. Input setting for hemodynamics of disturbed flow under dynamic shear

| Parameter	Symbol	Control Value
Cell radius (μm)	a_c	3.5
Characteristic Cell radius (μm)	a_{co}	3.5
Fluid dynamic viscosity (g/μm .sec)	μ	7×10^{-7}
Fluid density (g/μm³)	ρ	1×10^{-12}
Mass of the cell (g)	m	1.8×10^{-10}
Mass moment of inertia of the cell (g μm²)	I	8.82×10^{-10}
Characteristic receptor density (sites/μm²)	$[nR_{oo}]$	200
Receptor density (sites/μm²)	$[nR_o]$	200
Ligand density (sites/μm²)	$[nL_o]$	200
Bond stiffness (dyne/cm)	S	1.5×10^{-2}
Transition bond stiffness (dyne/cm)	S_{ts}	1.45×10^{-2}
Natural bond length (μm)	L_{bo}	0.011
Equilibrium bond formation rate constant (μm²/sites . sec)	K_{fo}	Changed from (0.08) to (0.016)
Equilibrium bond breakage rate constant (1/sec)	K_{bo}	Changed from (6.4) to (0.32)
Boltzmann's constant (J/°K)	K_B	1.381×10^{-23}
The temperature (°K)	T	310
Shear rate (s⁻¹)	G	Variable (-58.72 - 100)
Characteristic shear rate (s⁻¹)	G_o	100
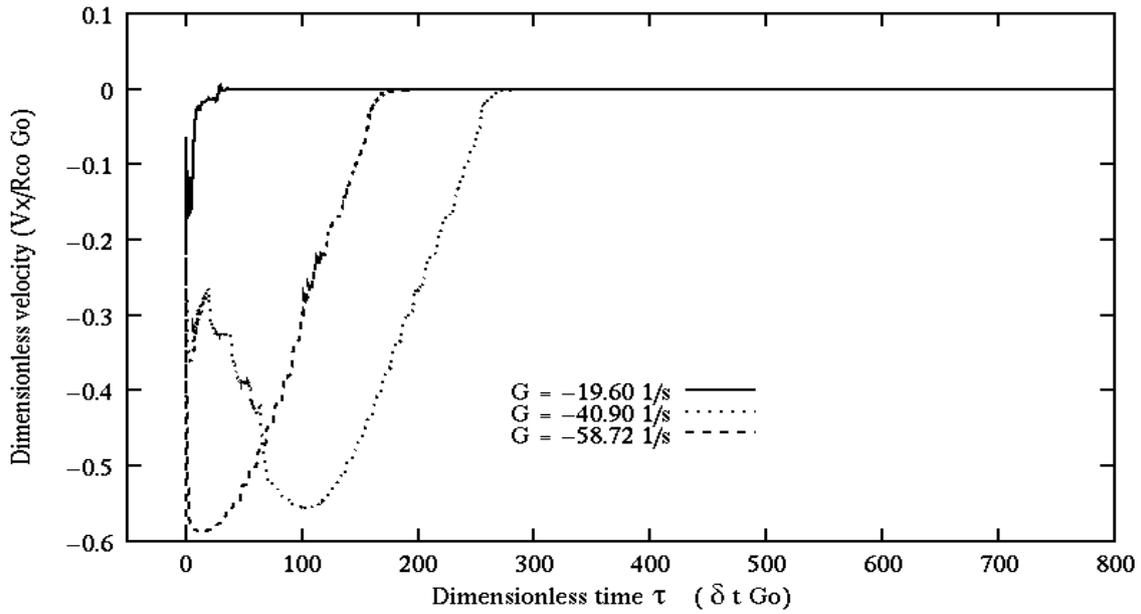
Figure 9. Cell capture and adhesion under range of negative shear rate (before the stagnation point location)
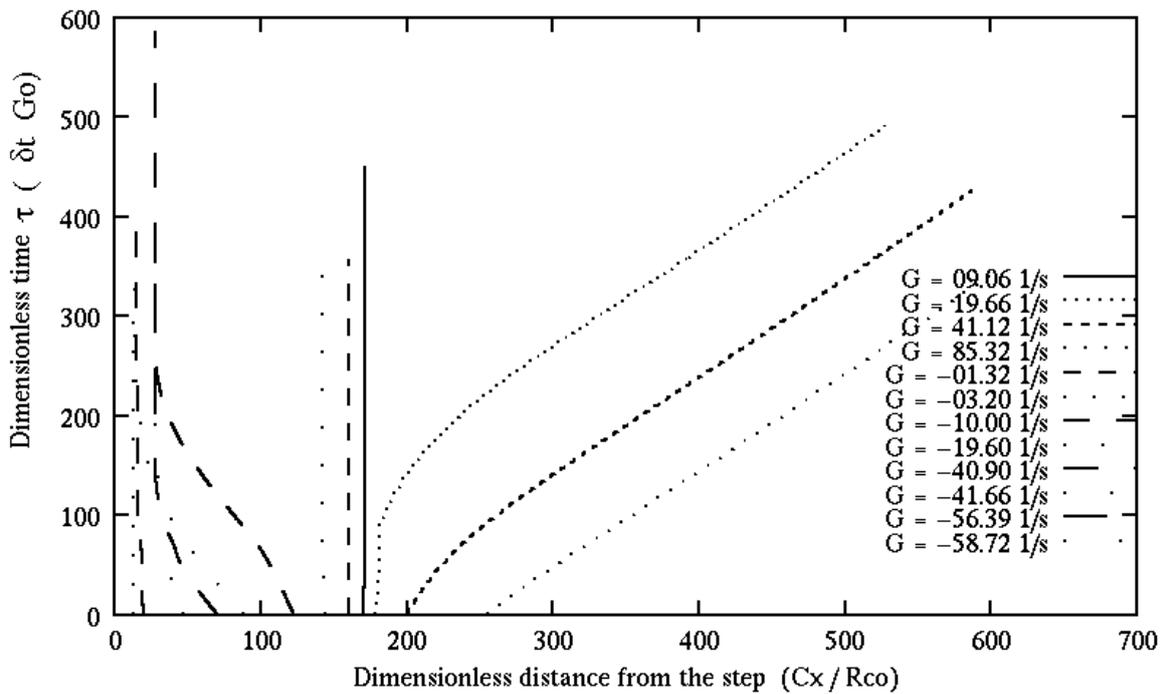

Figure 10. Cellular paths downstream the step (around the stagnation point) for different starting variable shear rate and different location from the step ($R_{co}= a_{co}$)

The present simulation was performed using relatively high site density and moderate site density, which means favorable conditions for adhesion. Mainly, the adhesion was dominant in the recirculation zone despite some rolling before the permanent arrest, while rolling has occurred -even under low shear rate- just at the far edge of recirculation zone (bit further the stagnation point). The short rolling downstream the step (recirculation zone) and fast rolling after the stagnation point can be explained by

the critical role of shear rate in cellular behavior within this area rather than the bond kinetics. Also, the rolling within the recirculation zone (low shear rate) is due to the rotational nature of flow (vortex) in this zone, where the shedding of vortices creates an oscillatory lift [20, 29, 30]. The shear rate in this type of flow had stronger effect than any other parameter, so it has strongly controlled the cellular behavior more than bond properties or site density. Accordingly, the results emphasizes that local fluid

dynamics (i.e., shear rate) of the complex flow plays a central role in cell adhesion and rolling within this type of flow, which dominant the other parameters roles [31].

In general, adhesion in the laminar re-established flow was as expected, being efficient at lower shear stress and negligible at higher rate. However, the lack of adhesion under low shear stress (downstream of the reattachment point) can be explained by the expansion of streamlines as they pass from narrower to wider conditions, so the cells effectively move away from the wall [28].

The above findings elucidate the details of cellular motion under disturbed flow, which can be used to explain cell adhesion under certain physiological conditions in the cardiovascular system. The pathophysiological implication of these results is that whereas adhesion may rarely occur in straight arteries, leukocyte could bind successfully in the region of a discontinuity. With regard to pathology, this may be a factor in localization of atheroma to low shear regions of vortices and recirculation associated with arterial junctions and curvature. Enhanced deposition could also influence process such as restenosis in vessels subjected to angioplasty, or thrombosis downstream of

anastomoses following surgical reconstruction of arteries [32].

5. Ranges of Adhesion and Rolling for Disturbed Flow under Variable Shear Rate

As an extension to the above analysis, more simulations were performed to determine the ranges of adhesion and rolling for disturbed flow under variable shear rate using data of Table 1 (Fig. 11).

In general, the analysis at this stage concentrate on the third step of cell adhesion and rolling, which is called 'secondary adhesion', 'permanent adhesion' or 'arrest'. This type of adhesion is the final stage in the cellular behavior over the wall of the vessel, in addition, it is the dominant event downstream the discontinuity in the flow (Figs. 10 & 11).

Start of secondary adhesion depends on the bio-physiochemical properties of the bond and on the conditions of flow, also the starting time of secondary adhesion determines the end of cell rolling stage, range of adhesion and the shear rate limit for fast rolling.
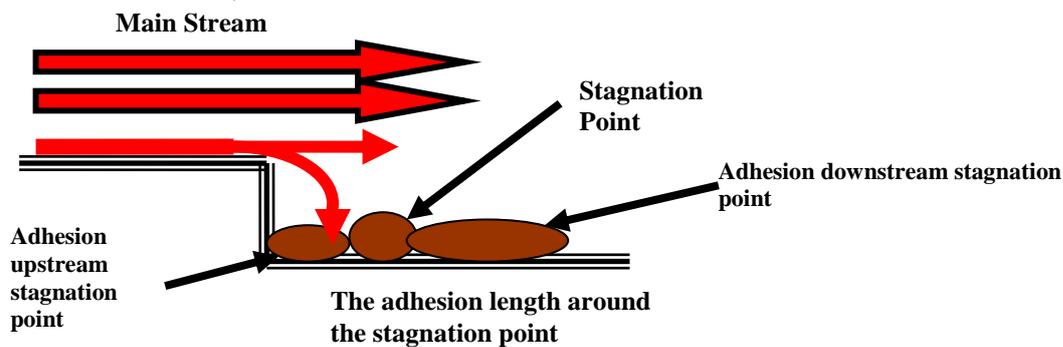

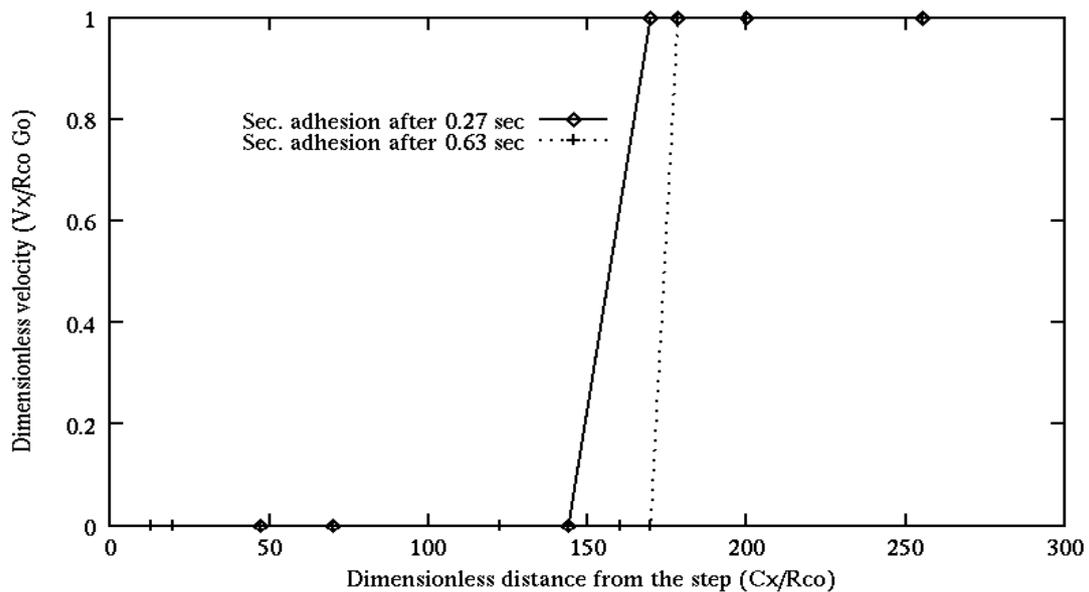**Figure 11.** Upstream and downstream stagnation point adhesion for disturbed flow conditions

Figure 12. Effect of secondary adhesion start on cell-surface interactions under variable shear rate

In this analysis, the adhesion lengths around the stagnation point have been determined for two different starts of secondary adhesion. Moreover, the shear limits for adhesion and fast rolling were specified and compared to show the effect of secondary adhesion start on cell motion. The results of this analysis are illustrated in Figs. 12 and 13.

Figure 12 demonstrates that as the secondary adhesion starts earlier (early activation of cells that have primary adhesive rolling) the adhesion length will be shorter, so the adhesion length was within $6.0 \le C_x/a_c \le 144.0$ (i.e., length of 483 μm), and fast rolling started at $C_x/a_c = 169.7$ (i.e., at $C_x \approx 594$ μm) when the secondary adhesion started at 0.27 sec. However, longer adhesion length was at later start of secondary adhesion (later activation of primary rolling cells). The adhesion was within $6.0 \le C_x/a_c \le 169.7$ (i.e., length of 594 μm) at the secondary adhesion start of 0.63 sec., while the fast rolling started at $C_x/a_c = 178.28$ (i.e., at $C_x \approx 624$ μm). It can be noted that the adhesion in this case was on both sides of the stagnation point as it is located at $C_x/a_c = 162.0$.

Figure 13 shows the shear ranges for adhesion and rolling for secondary adhesion starts of 0.27 and 0.63 sec respectively. For 0.27 sec start, adhesion was taken place up to G/G_o of -0.196 (i.e., $G = -19.60$ s^{-1} & $C_x = 144$ μm) and the fast rolling limit was at G/G_o of 0.0906 (i.e., $G = 9.06$ s^{-1} & $C_x = 169.7$ μm).

On the other hand, at 0.63 sec, they were G/G_o of 0.0906 (i.e., $G = 9.06$ s^{-1}, $C_x = 169.7$ μm) for end limit of adhesion and G/G_o of 0.196 (i.e., $G = 19.60$ s^{-1} & $C_x = 178.28$ μm) for begin of fast rolling. This means that delay in starting of the secondary adhesion (delay of activation) allows the bonds to withstand more effect of drag force, and causes late cell rolling. Moreover, when the cell had long adhesive rolling under increasing shear rate before its secondary adhesion (late secondary adhesion start), the bond formation will be promoted to maintain the adhesive nature rolling. So when the secondary adhesion starts

under these conditions, another factor is added to support adhesion in the opposite of shear rate, which enable for longer adhesion length and delay fast rolling.

6. Conclusion

It is possible to determine cell adhesion location ranges, adhesion length and rolling limits for disturbed flow under variable shear rate. In addition, the adhesion length will be longer and on both sides of the stagnation point if the cell starts its secondary adhesion in a while, even though at higher shear rate. However, when the cell starts its secondary adhesion earlier, the adhesion will be shorter and mainly concentrated before the stagnation point, while rolling is dominant beyond this point.

These findings can be used to explain the cellular behavior (i.e., cell adhesion) at junctions, bifurcation and stenosis in the cardiovascular arteries. Also, clear idea can be obtained about cell type in regarding to its permanent adhesion, its ability to support adhesion/rolling and its kinetic activity (rates of bond formation and breakage) by analyzing the ranges of adhesion and rolling.

Another important point can be mentioned here, cell adhesion and rolling can be considerably controlled by secondary adhesion start technique. It is possible to extend or limit the ranges of cell adhesion or rolling under the same conditions of flow, by alteration of K_{bo}^- and K_{fo}^+, which means different type of bonds, furthermore, the timing of secondary adhesion has a particular role in cell motion. However, secondary adhesion can be also achieved using the same type of bonds, by changing of the site density or shear rate.

Finally, it is significant to remember that this technique can be employed to get more stable or low rolling under high shear rate or low site density to study the cell motion under wide ranges of parameters or more complicated flow conditions.
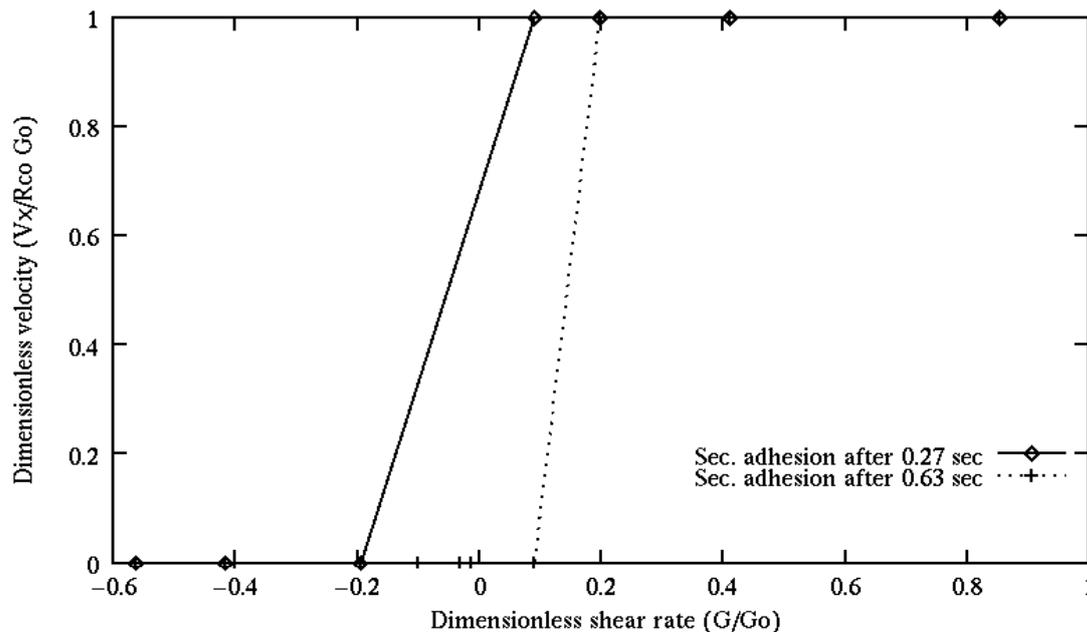

Figure 13. Effect of secondary adhesion start on shear rate limit for adhesion under variable shear rate

References

[1] Hammer, D. A., and Apte, S. M., "Simulation of cell rolling and adhesion on surfaces in shear flow: general results and analysis of selectin-mediated neutrophil adhesion," Biophys. J. 63, 1992, pp. 35-57.

[2] Hammer, D. A. and Lauffenburger, D. A., "A dynamic model for receptor-mediated cell adhesion to surfaces," Biophy. J. 52, 1987, pp. 457-487.

[3] Schmidtke, D. W., & Diamond, S. L., Direct observation of membrane tethers formed during neutrophil attachment to platelets or P-selectin under physiological flow, The Jor. of Cell Biology, Vol. 149, May 2000, 719-729.

[4] Lei, X., Lawrence, M. B., & Dong, C., "Influence of cell deformation on leukocyte rolling adhesion in shear flow," J. of Biomechanical Engineering, ASME, Vol. 121, 1999, pp. 636-643.

[5] Chen, S., & Springer T. A., "An automatic braking system that stabilizes leukocyte rolling by an increase in selectin bond number with shear." The J. of Cell Biology, Jan., Vol. 144, No.1, 1999. pp. 185-200.

[6] Shao, J., Ting-Beall, H., & Hochmuth, R., "Static and dynamic lengths of neutrophil microvilli," Proc. Natl. Acad. Sci., USA, , Vol. 95, 1998, pp. 6797-6802

[7] Malek, A. M., & Izumo S., Mechanism of endothelial cell shape change and cytoskeletal remodeling in response to fluid shear stress, J. of Cell Science, 109, 1996, 713-726.

[8] Abueg, E., The Effects of Flow on Adhesion Molecule Expression and Monocyte-Endothelial Interactions In Vitro, Ph.D. thesis, Rensselaer Polytechnic Institute, Troy, New York, 2008 http://proquest.umi.com/pqdlink?did=1746891101&Fmt=14 &VType=PQD&VInst=PROD&RQT=309&VName=PQD& TS=1274706241&clientId=79356

[9] Ravensbergen J. W. ; Krijger J. K,. Hillen B., Hoogstraten H. W., "Localizing role of hemodynamics in atherosclerosis in several human vertebrobasilar junction geometries," Arterioscler Thromb Vasc Biolg.; 18, 1998, pp. 708-716.

[10] Swift, D. G., Posner, R. G., & Hammer, D. A., Kinetics of adhesion of IgE-sensitized rat basophilic leukaemia cells to surface-immobilized Antigen in Couette flow, Biophs. J., Vol. 75, 1998, 2597-2611.

[11] Bell, G. I., "Models for specific adhesion of cells to cells, Science," Vol. 200, 1978, pp. 618-627.

[12] Dembo, M., Torney, D. C., Saxman, K., and Hammer D., "The reaction-limited kinetics of membrane-to-surface adhesion and detachment," Proceeding R. Soc. London, B234, 1988, pp. 55-83.

[13] Krasik, E. F., Adhesive Dynamics Simulation of Neutrophil Arrest with Deterministic Activation, Biophysical. J. 91, 2006, 1145-1155.

[14] Krasik, E. F., and Daniel A. Hammer, A Semianalytic Model of Leukocyte Rolling, Biophysical. J. 87, 2004, 2919-2930.

[15] http://mitocw.udsm.ac.tz/NR/rdonlyres/5059F757-7204-45F4-9409-EDC762C28456/0/lec_25_slides.pdf

[16] Goldman, A. J., Cox, R. G., and Brenner, H., "Slow viscous motion of a sphere parallel to a plane wall- I. Motion through a quiescent fluid," Chemical Engineering Science, 22, 1967, pp. 637-651.

[17] Goldman, A. J., Cox, R. G., and Brenner, H., "Slow viscous motion of a sphere parallel to a plane wall- II. Coutte flow," Chemical Engineering Science, 22, 1967, pp 653-660.

[18] King, M., R., and Hammer, D., Multiparticle Adhesive Dynamics Interactions between Stably Rolling Cells, Biophysical journal, 81, 2001, 799-813.

[19] Lawrence, M. B., and Springer, T. A., "Leukocytes roll on a selectin at physiologic flow rates: distinction from and prerequisite for adhesion through integrins," Cell, 56, 1991, pp. 859-873.

[20] Dinnar, U., "Cardiovascular fluid dynamics", CRC press, Inc. Florida, USA, 1981

[21] Bausch A. R., Moller, W., & Sackmann, E., Measurement of local viscoelasticity and forces in living cells by magnetic tweezers, Biophys. J. Vol. 76, Jan. 1999, 573-579.

[22] Chang, K., Tees, D. F. J., & Hammer, D. A., The state diagram for cell adhesion under flow: Leukocyte rolling and firm adhesion, Proc. Natl. Acad. Sci., USA, Vol. 97, No. 21, Oct. 2000, 11262-11267.

[23] Cozens-Roberts, C., Quinn, J. A., and Lauffenburger, D. A., "Receptor-mediated adhesion phenomena-model studies with radial detachment assay," Biophys. J. 58, 1990, pp.107-125.

[24] Alon, R., Chen, S., Puri, K. D., Finger, E. B., & Springer, T. A., "The kinetics of L-selectin tethers and the mechanics of selectin-mediated rolling," The J. of Cell Bio. Vol. 138, No.5, 1997, pp. 1169-1180.

[25] Tozeren, A. and Ley, K., How do selectins mediate leukocyte rolling in venules? Biophys. J. 63, 1992, 700-709.

[26] Sinnott, M., Cleary, P. W., and Prakash, M., 2006, AnInvestigation of Pulstile Blood Flow in A Bifurcation Artery Using a Grid-Free Method, Fifth International Conference on CFD in the Process Industries, CSIRO, Melbourne,13-15-Dec. 2006, Australia- URL: http://www.cfd.com.au/cfd_conf06/PDFs/119Sin.pdf

[27] http://www.bakker.org/dartmouth06/engs150/11-bl.pdf @ 20/5/2010

[28] Skilbeck, C.,Westwood, S.M., Walker, P.G., David,T., and Nash, G.B., "Dependence of adhesive behaviour of neutrophils on local fluid dynamics in a region with recirculating flow," Biorheology, 38 (2-3), 2001, pp. 213-227.

[29] Fung, Y. C., "Biomechanics: Motion, flow, stress and growth", Spirnger-Verlag, New York, Inc. USA, 1990.

[30] Massey, B. S., "Mechanics of fluids", 6th ed., Chapman & Hall, London, UK, 1988.

[31] Chiu, J. J., Wang, D. L., Chien, S., Skalak, R., and Usami, S., "Effects of Distributed flow on endothelial cells", J. Biomechanical Engineering, Vol.120, 1998, pp.2-8.

[32] Skilbeck, C.,Westwood, S.M., Walker, P.G., David,T., and Nash, G.B., "Population of the vessel wall by leukocytes binding to P-selectin in a model of disturbed arterial flow", Arterioscler Throm Vasc Bio, 21, 2001, pp. 1294-1300.